Supporting Information for

Bimetallic NiFe/Al_2O_3 Catalyst for Efficient Hydrogenolysis of Polyethylene into Aviation Fuel Range Alkanes

Rongfei Cong,[a] Jiahui Zhan,[b, c] Ruihong Dai,[b] Hu Luo,[b*] Haozhi Zhou,[a] Lin Xia,[b] Hui Wang[a,b,d*]

[a] Institute of Carbon Neutrality, ShanghaiTech University, Shanghai 201203, People's Republic of China.

[b] CAS Key Laboratory of Low-Carbon Conversion Science and Engineering, Shanghai Advanced Research Institute, Chinese Academy of Sciences, Shanghai 201210, People's Republic of China.

[c] Shanghai Technical Service Platform for Pollution Control and Resource Utilization of Organic Wastes, Shanghai Key Laboratory of Atmospheric Particle Pollution and Prevention (LAP3), Department of Environmental Science and Engineering, Fudan University, Shanghai 200438, People's Republic of China.

[d] Shanghai Institute of Cleantech Innovation, Shanghai 201616, People's Republic of China.

*Corresponding authors:

E-mail address: luoh@sari.ac.cn; wanghh@sari.ac.cn

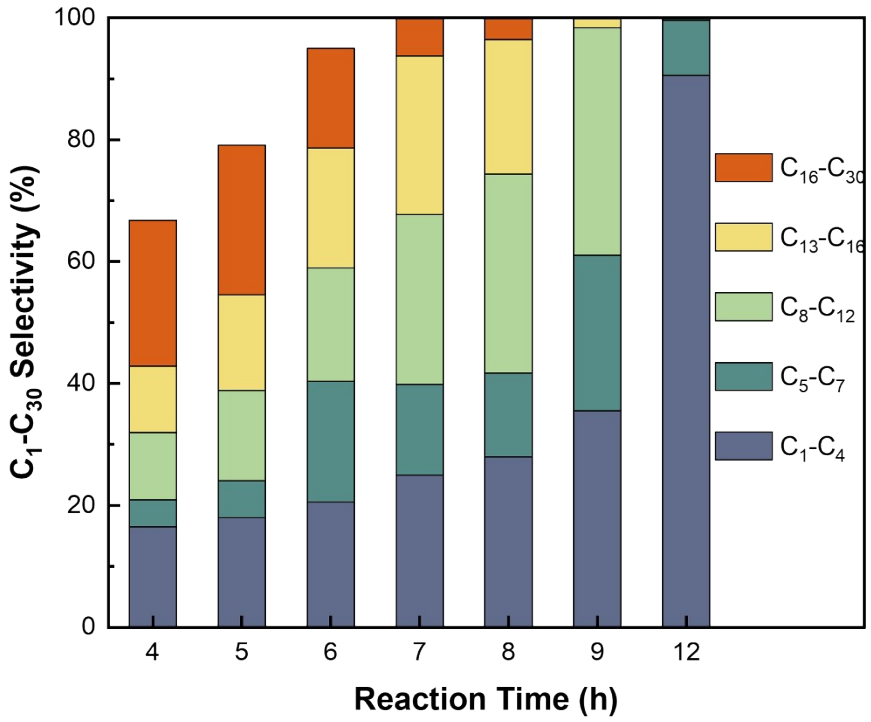

Figure S1 Time effect on LDPE hydrogenolysis liquid product distributions (2 g LDPE, 0.1 g 10Ni/Al_2O_3, 300°C, 3 MPa H_2).

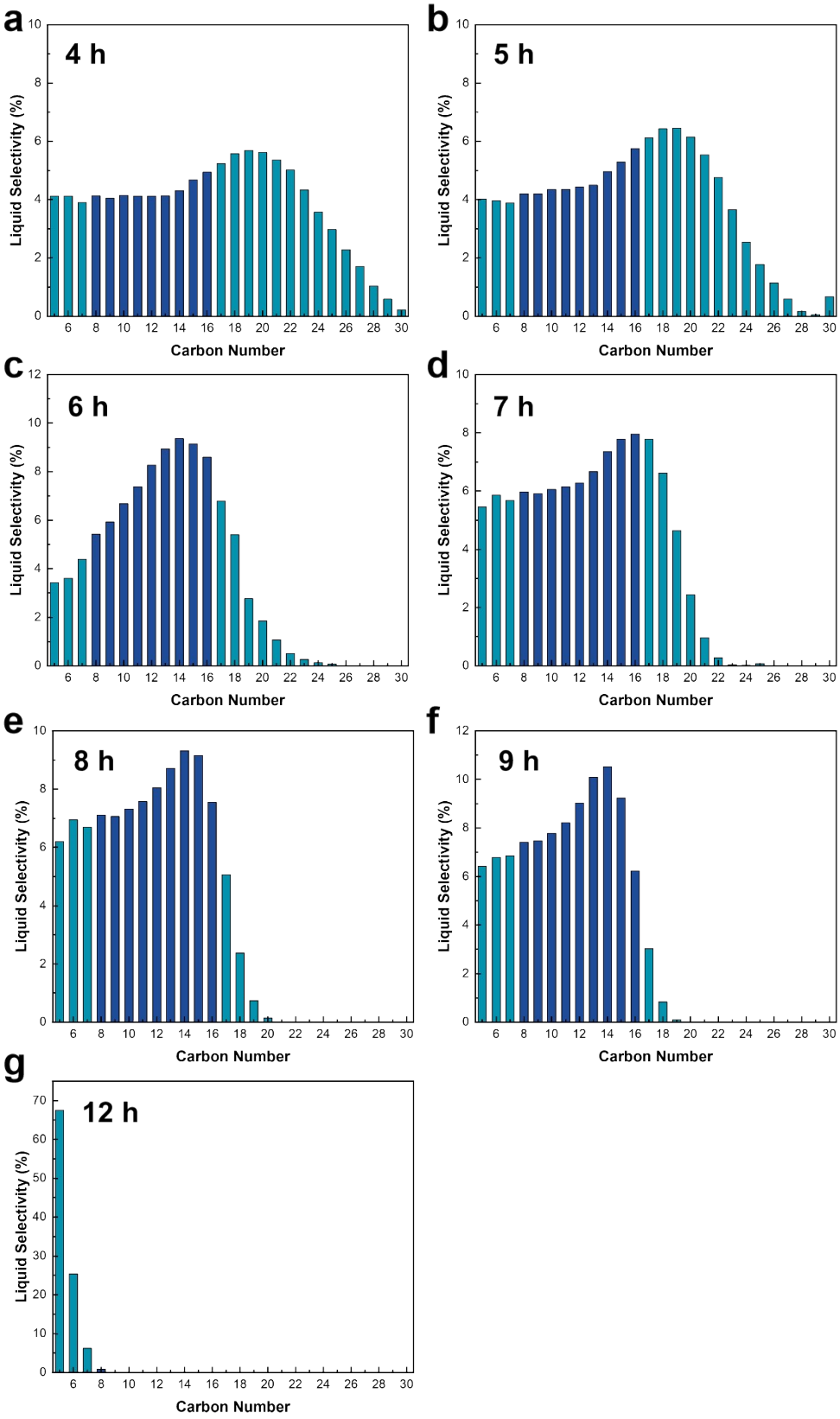

Figure S2 Carbon distributions of liquid products (2 g LDPE, 0.1 g 10Ni/Al_2O_3, 300°C, 3 MPa H_2)**.** (a) 4 h, (b) 5 h, (c) 6 h, (d) 7 h, (e) 8 h, (f) 9 h, (g) 12 h.

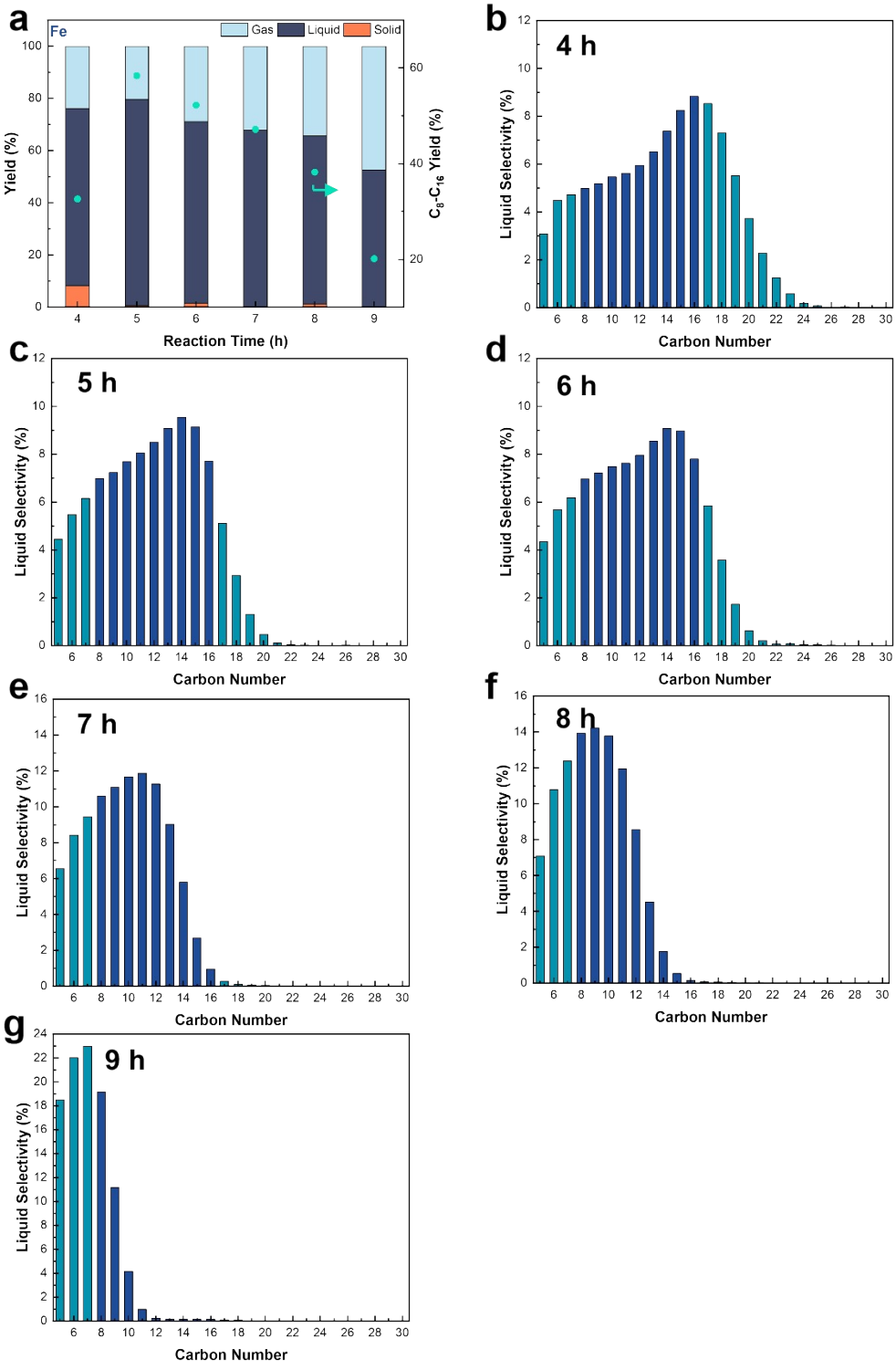

Figure S3 Time effect on LDPE hydrogenolysis liquid product distributions (2 g LDPE, 0.1 g 10Ni2Fe/Al_2O_3, 300°C, 3 MPa H_2)**.** (a) 4 h, (b) 5 h, (c) 6 h, (d) 7 h, (e) 8 h, (f) 9 h.

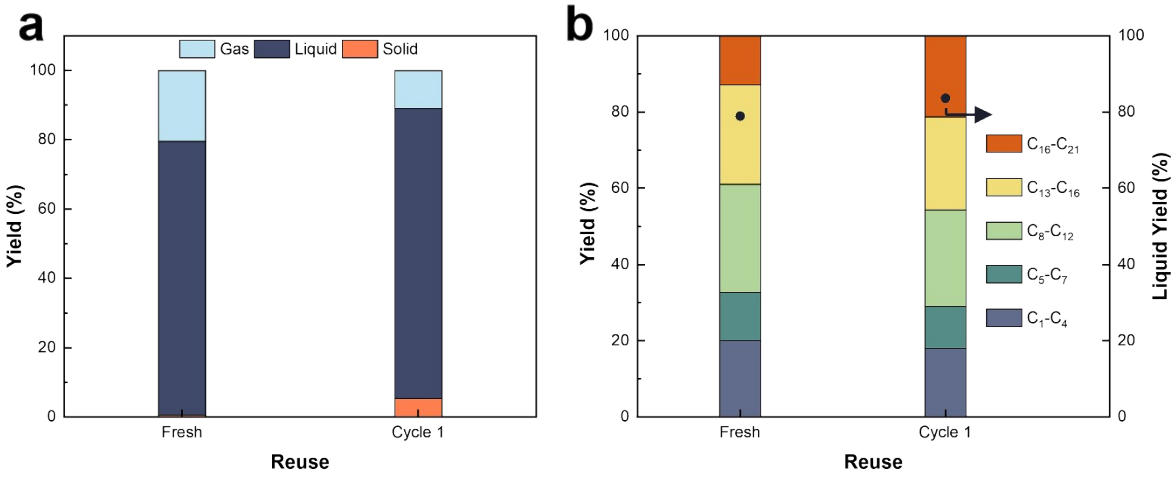

Figure S4 Recyclability of 10Ni2Fe/Al_2O_3 for LDPE hydrogenolysis. (a) Overall product yields distributions of cycles, (b) Product distributions.

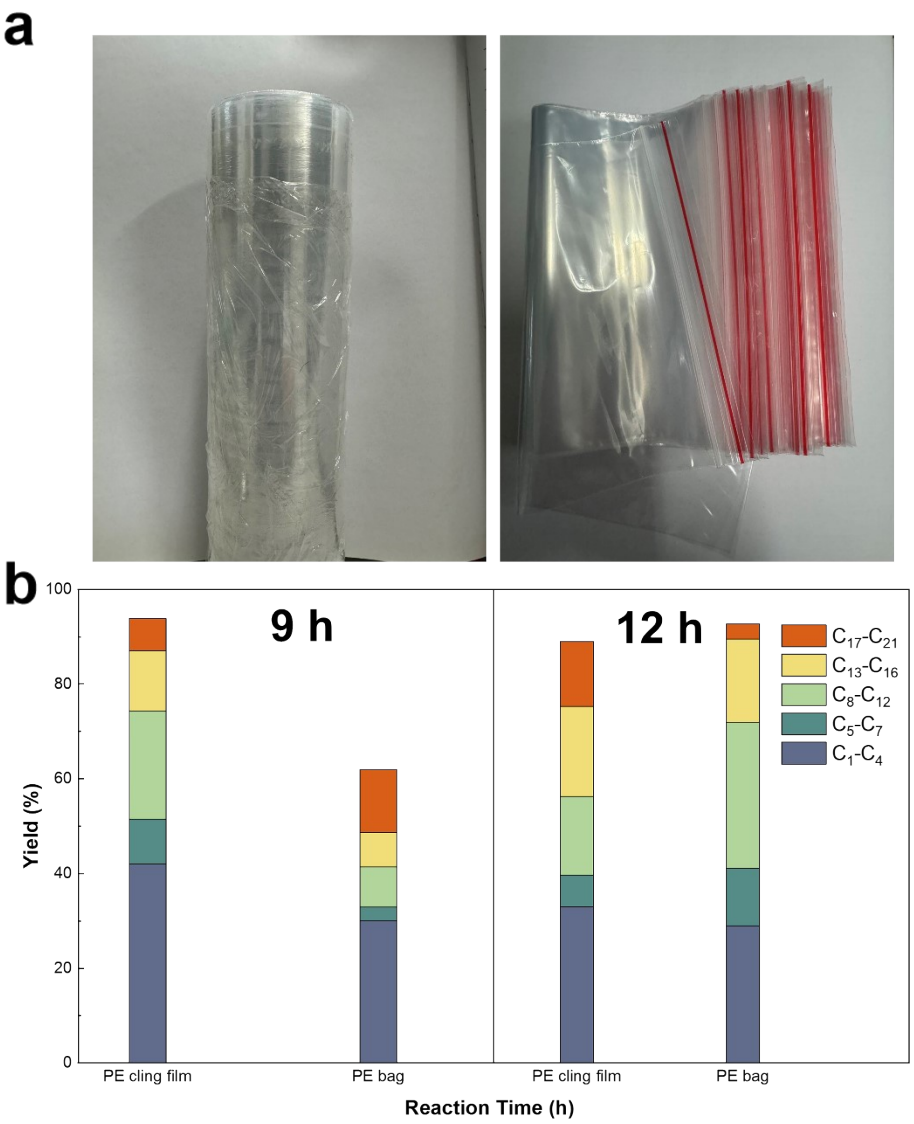

Figure S5 Hydrogenolysis of real plastic. (a) Illustration of different real plastics used in (b), (b) Product distribution over 10Ni2Fe/Al_2O_3 catalyst(1.0 g plastic, 0.1 g catalyst, 300 °C, 3 MPa H_2)

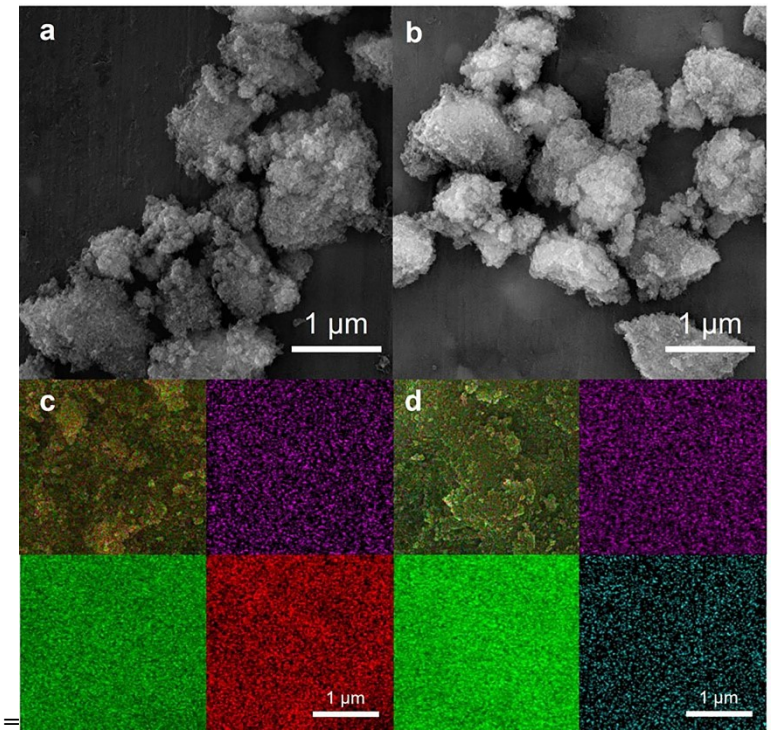

Figure S6 SEM images and EDS Mapping of 10Ni2Fe/Al_2O_3 and 10Ni/Al_2O_3 catalysts. (a,b) SEM images of 10Ni/Al_2O_3 and 10Ni2Fe/Al_2O_3, (c,d) EDS Mapping of 10Ni/Al_2O_3 and 10Ni2Fe/Al_2O_3. The color originated from the combination of purple (Ni), green (Al), cyan(Fe) and red(O).

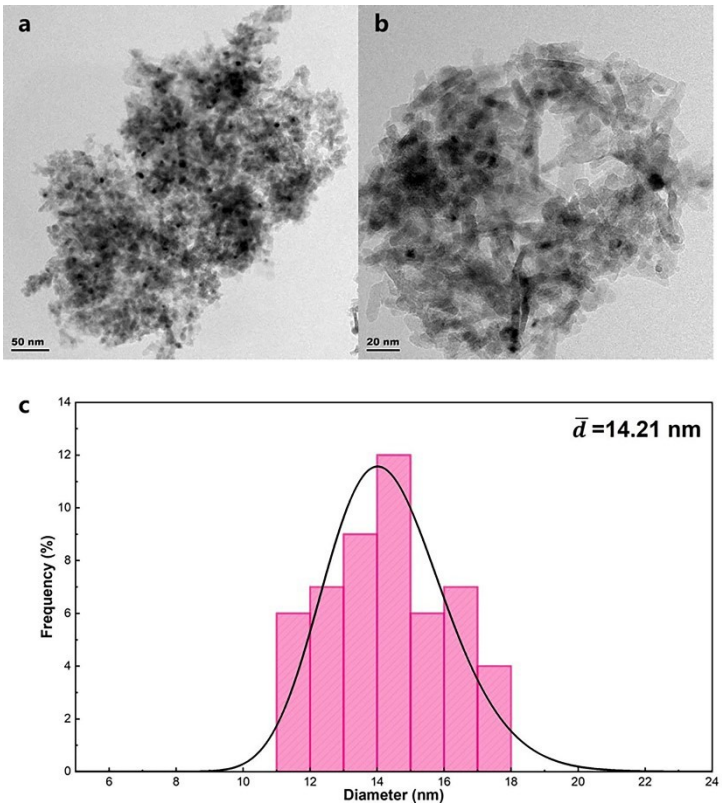

Figure S7 TEM images of the 10Ni/Al_2O_3 catalysts. (a,b) TEM Images, (c) Particle size distribution.

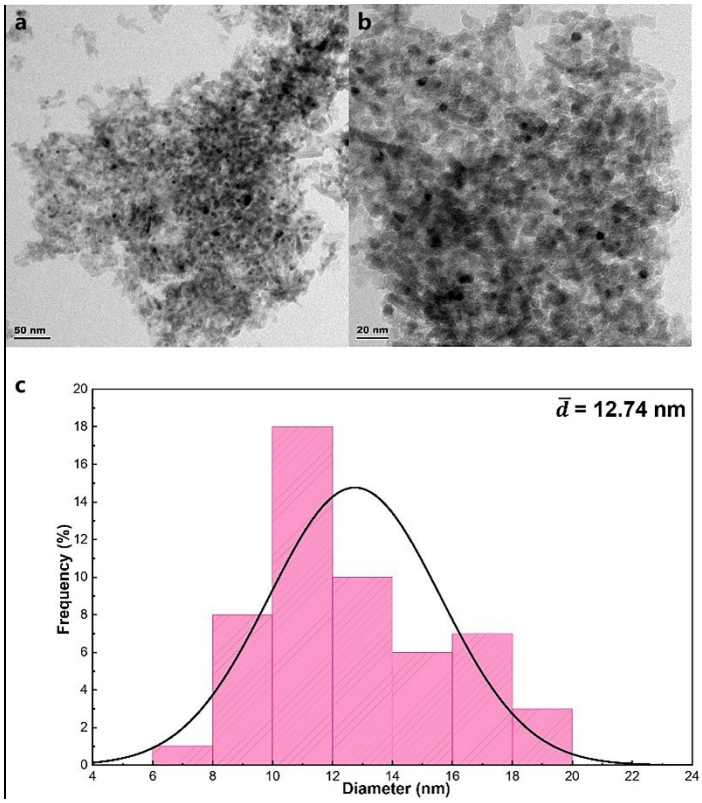

Figure S8 TEM images of the 10Ni2Fe/Al_2O_3 catalysts. (a,b) TEM Images, (c) Particle size distribution.

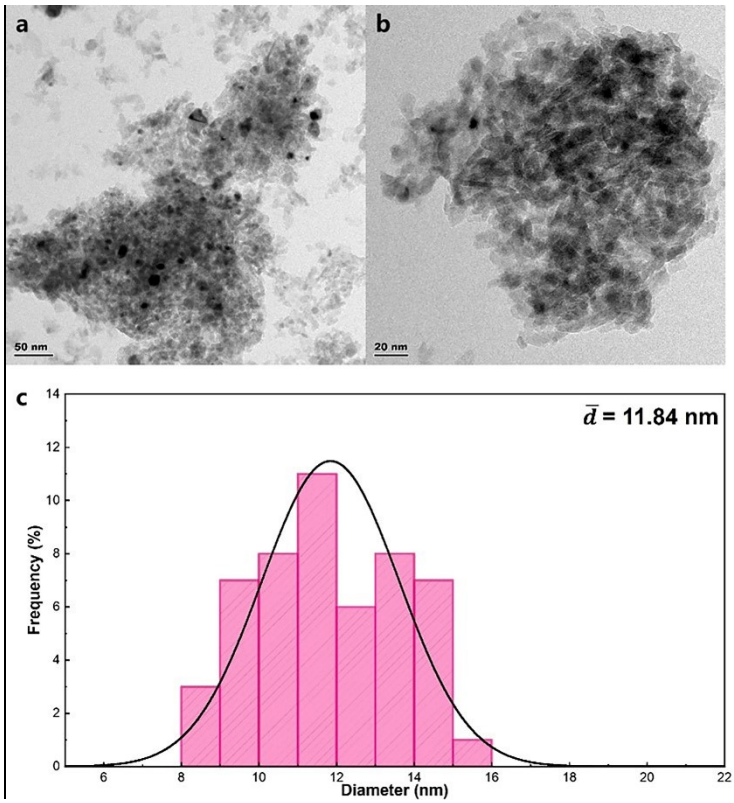

Figure S9 TEM images of the 10Ni5Fe/Al_2O_3 catalysts. (a,b) TEM Images, (c) Particle size distribution.

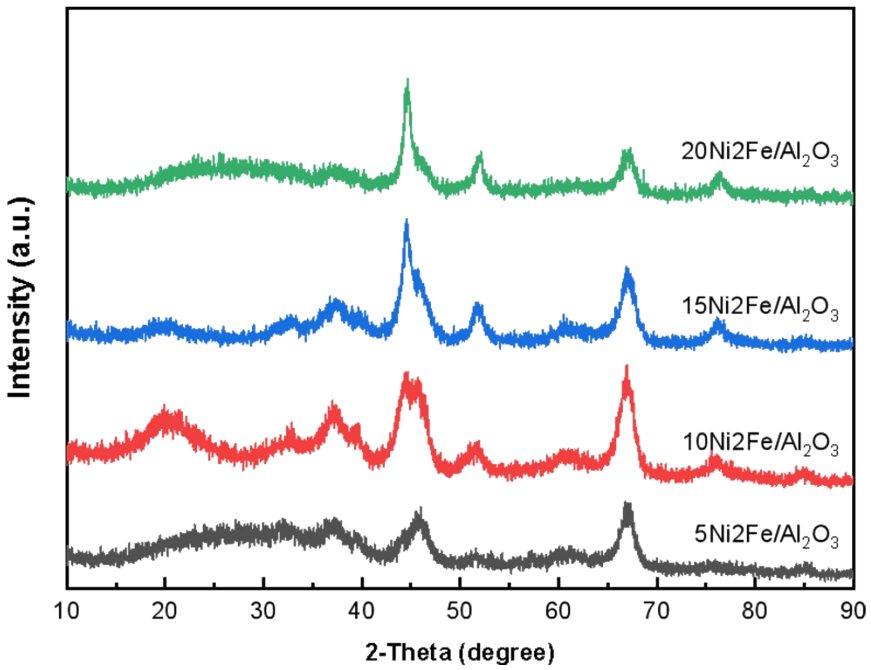

Figure S10 XRD patterns of $NiFe/Al_2O_3$ catalysts.

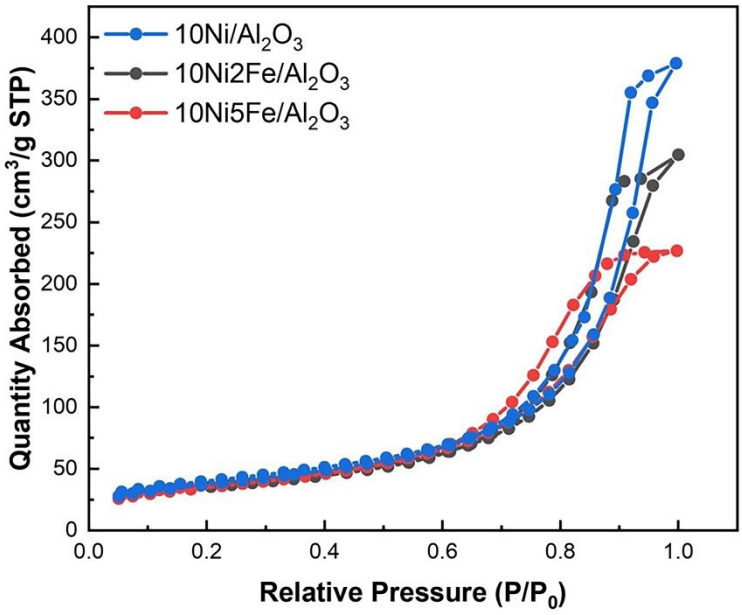

Figure S11 The N_2 adsorption isotherms of $NiFe/Al_2O_3$.

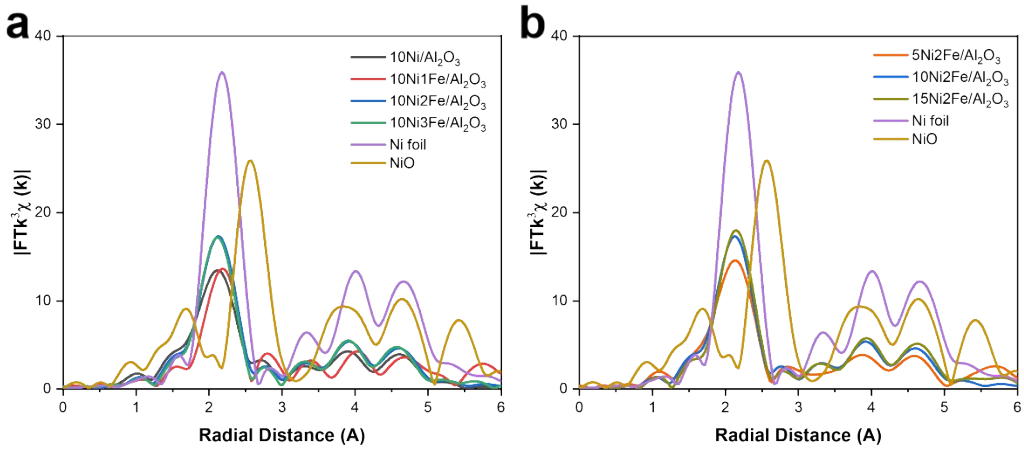

Figure S12 k^3-weighted Fourier transforms of Ni K-edge EXAFS spectra with different metal loadings.

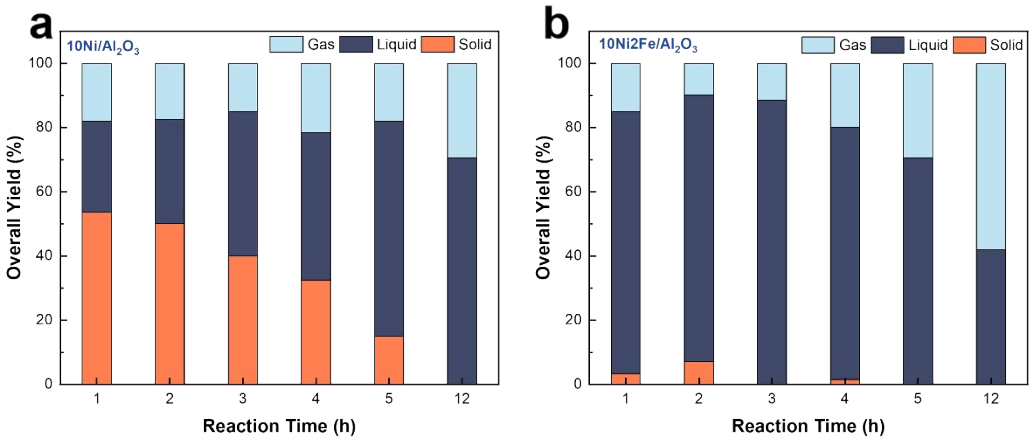

Figure S13 Product distributions for C_{28} hydrogenolysis with different catalysts (2 g C_{28}, 0.1 g catalyst, 300 °C, 3 MPa H_2). (a) 10Ni/Al_2O_3, (b) 10Ni2Fe/Al_2O_3.

Table S1. Ni and Fe loading measured by icp

Sample	Ni(%)	Fe(%)
10Ni2Fe/Al_2O_3	9.43	1.6
10Ni5Fe/Al_2O_3	9.84	4.25
5Ni/Al_2O_3	4.62	
10Ni/Al_2O_3	9.33	
15Ni/Al_2O_3	13.93	
20Ni/Al_2O_3	18.27	

Table S2. Analysis of different Ni-based catalysts

Sample	BET surface area(m^2/g)	Pore Volume(cm^3/g)	Pore Size(nm)
5Ni/Al_2O_3	159.36	0.74	18.54
10Ni/Al_2O_3	140.70	0.59	16.66
15Ni/Al_2O_3	128.53	0.49	15.20
20Ni/Al_2O_3	133.56	0.40	11.95
10Ni2Fe/Al_2O_3	129.67	0.43	14.54
10Ni5Fe/Al_2O_3	129.94	0.35	10.80